17. W. M. Shih, J. D. Quispe, G. F. Joyce, *Nature* **427**, 618 (2004).
18. P. W. Rothemund, *Nature* **440**, 297 (2006).
19. S. M. Douglas *et al.*, *Nature* **459**, 414 (2009).
20. S. M. Douglas *et al.*, *Nucleic Acids Res.*; published online 16 June 2009 (10.1093/nar/gkp436).
21. J. C. Mitchell *et al.*, *J. Am. Chem. Soc.* **126**, 16342 (2004).
22. C. Lin *et al.*, *Nano Lett.* **9**, 433 (2009).
23. K. Luger *et al.*, *Nature* **389**, 251 (1997).
24. J. A. Borowiec *et al.*, *J. Mol. Biol.* **196**, 101 (1987).
25. J. Chang *et al.*, *Structure* **14**, 1073 (2006).
26. H. G. Garcia *et al.*, *Biopolymers* **85**, 115 (2007).
27. S. C. J. Parker, L. Hansen, H. O. Abaan, T. D. Tullius, E. H. Margulies, *Science* **324**, 389 (2009); published online 12 March 2009 (10.1126/science.1169050).


28. H.D. thanks Andres E. Leschziner for training in electron microscopy and generous supply of image processing hardware and software. This work was supported by Claudia Adams Barr Program Investigator, Wyss Institute for Biologically Inspired Engineering, and NIH New Innovator (1DP2OD004641-01) grants to W.M.S. and a Feodor-Lynen Humboldt Fellowship to H.D. H.D., S.M.D., and W.M.S. designed the research for this paper. H.D. developed rules for twisting and bending; H.D. and S.M.D. designed all shapes; H.D. and S.M.D. collected data; H.D. analyzed data; S.M.D. provided caDNAno software support; and H.D., W.M.S., and S.M.D. wrote the manuscript.


**Supporting Online Material**
www.sciencemag.org/cgi/content/full/325/5941/725/DC1
Materials and Methods
SOM Text
Figs. S1 to S26
References


30 March 2009; accepted 25 June 2009
10.1126/science.1174251


# Unexpected Epoxide Formation in the Gas-Phase Photooxidation of Isoprene


**Fabien Paulot,[1]* John D. Crounse,[2] Henrik G. Kjaergaard,[3,4] Andreas Kürten,[1]† Jason M. St. Clair,[1] John H. Seinfeld,[1,2] Paul O. Wennberg[1,5]**



**Emissions of nonmethane hydrocarbon compounds to the atmosphere from the biosphere exceed those from anthropogenic activity. Isoprene, a five-carbon diene, contributes more than 40% of these emissions. Once emitted to the atmosphere, isoprene is rapidly oxidized by the hydroxyl radical OH. We report here that under pristine conditions isoprene is oxidized primarily to hydroxyhydroperoxides. Further oxidation of these hydroxyhydroperoxides by OH leads efficiently to the formation of dihydroxyepoxides and OH reformation. Global simulations show an enormous flux—nearly 100 teragrams of carbon per year—of these epoxides to the atmosphere. The discovery of these highly soluble epoxides provides a missing link tying the gas-phase degradation of isoprene to the observed formation of organic aerosols.**


Isoprene is the largest source of nonmethane hydrocarbons to the atmosphere (~500 Tg C/year) (*1*). It is produced by deciduous plants (*2*) and plays a critical role in tropospheric chemistry over large regions of the globe (*3*). In many forested regions, isoprene oxidation by OH occurs far from combustion of biomass and fossil fuel, so nitric oxide (NO) concentrations are very low. Many of the details of the chemical oxidation mechanism under these conditions remain to be elucidated, hindering assessment of the consequences of changes in isoprene emissions from land use and climate variation (*1*, *4*–*6*) or changes in NO emissions. In addition to the uncertainty in the gas-phase chemistry, there is no agreement on the mechanism involved in the formation of secondary organic aerosol (SOA) from isoprene oxidation (*7*).

Where NO is low, isoprene photooxidation is expected to yield the hydroxyhydroperoxides, ISOPOOH = β-ISOPOOH + δ-ISOPOOH (Reaction Series 1, A and B) (*8*, *9*). These series of reactions are expected to strongly depress the concentrations of OH and $HO_2$ (together known as $HO_x$) in regions with high isoprene emissions. Observed $HO_x$ levels remain, however, almost unchanged over a wide range of isoprene concentrations, inconsistent with the simulated influence of Reaction Series 1, A and B (*10*–*12*). Simulations and measurements of $HO_x$ have been partly reconciled with substitution of the speculative Reaction Series 1C, where formation of methacrolein (MACR) and formaldehyde is accompanied by OH formation, thus reducing the impact of isoprene on $HO_x$ levels (*11*).

Analogous to Reaction Series 1, A to C, addition of OH on the other double bond yields similar hydroxyhydroperoxides (β1- and δ1-ISOPOOH) and methylvinylketone (MVK) (*13*). Both unimolecular decomposition of the peroxy radical (*14*) and reaction with $HO_2$ (*15*) have been proposed in Reaction Series 1C. Although OH reformation (15 to 65%) has been measured for the reactions of $HO_2$ with acylperoxy and β-carbonyl peroxy radicals, low OH yields (<6%) have been reported from the reactions of $HO_2$ with β-hydroxy peroxy radicals, structurally more similar to isoprene peroxy radicals (*15*).

We show here that ISOPOOH is formed in large yields (>70%) via the channels shown in Reaction Series 1, A and B, with concomitant formation of MVK and MACR in much smaller yields (<30%) via the channel shown in Reaction Series 1C. The branching through Reaction Series 1C yields OH, although substantially less than required to close the $HO_x$ budget (*11*).

We show below that the oxidation of ISOPOOH by OH produces dihydroxyepoxides (IEPOX = β-IEPOX + δ-IEPOX). This $HO_x$ neutral mechanism produces IEPOX with yields exceeding 75% (Reaction Series 2, A and B). This mechanism is likely specific to isoprene and other polyalkenes. Analogous to liquid phase processes (*16*), it profoundly differs from gas-phase oxidation of simple alkenes by OH (e.g., Reaction Series 1, A and B), which would result in the formation of the dihydroxydihydroperoxides. Formation of these compounds is not observed in these experiments.

The gas-phase formation of IEPOX in high yields provides a suitable gas-phase precursor for Secondary Organic Aerosol from isoprene oxidation (*i*SOA) under low-$NO_x$ conditions (*17*–*19*) and may help resolve an outstanding puzzle in atmospheric aerosol chemistry. Although epoxides have previously been speculated as a possible precursor for *i*SOA (*17*), no mechanism was known to produce them in either the gas or aerosol phase. Consistent with expectation that IEPOX can serve as a precursor to *i*SOA, we

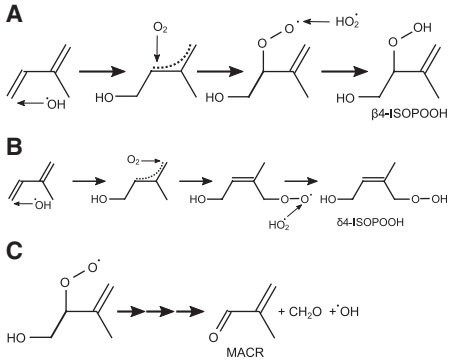


**Reaction Series 1.**

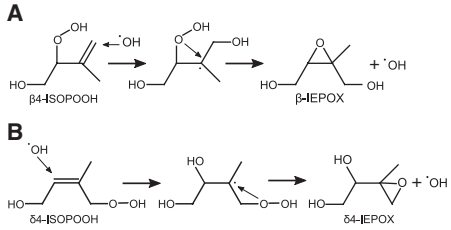


**Reaction Series 2.**


[1]Division of Engineering and Applied Science, California Institute of Technology, Pasadena, CA 91125, USA. [2]Division of Chemistry and Chemical Engineering, California Institute of Technology, Pasadena, CA 91125, USA. [3]Department of Chemistry, University of Otago, Dunedin, New Zealand. [4]Department of Chemistry, University of Copenhagen, Copenhagen, Denmark. [5]Division of Geological and Planetary Sciences, California Institute of Technology, Pasadena, CA 91125, USA.

*To whom correspondence should be addressed. E-mail: paulot@caltech.edu

†Present address: Institute for Atmospheric and Environmental Sciences, Goethe University, Frankfurt am Main, Germany.


Downloaded from http://science.sciencemag.org/ on January 15, 2017

observe rapid and quantitative uptake of 1,4-dihydroxy-2,3-epoxybutane (BEPOX)—a compound structurally similar to IEPOX—on acidic aerosol.

We monitor isoprene photooxidation products in the Caltech environmental chamber by chemical ionization mass spectrometry (CIMS) (*20*), employing a triple-quadrupole mass filter that provides tandem mass spectra (MSMS) (*13*). The reagent anion, $CF_3O^-$, provides sensitive detection of organic hydroperoxides by formation of ion-molecule clusters (*20*). Detection of BEPOX by CIMS confirms its sensitivity to dihydroxy-epoxides (*13*). In the absence of native standards for many of the compounds described here, the calibration of the instrument was inferred from molecular properties of the analyte (*13*, *21*).

Isoprene is oxidized by OH generated through the photolysis of hydrogen peroxide ($H_2O_2$) in a Teflon bag filled with 800 standard liters of ultra-zero air. Known amounts of isoprene and $H_2O_2$ are introduced into the chamber before ultraviolet (UV) lights are energized. Isoprene is quantified using gas chromatography with flame ionization detection (GC-FID) (*13*).

The products formed through Reaction Series 1, A and B, and Reaction Series 2, A and B—ISOPOOH and IEPOX—are isobaric and measured together by CIMS as the cluster of $CF_3O^-$ with these compounds at the mass to charge ratio (*m/z*) 203 (Fig. 1, red curve). However, distinct daughter ions produced through collision-induced dissociation (CID) of these cluster ions allow for quantification of each compound (*22*). Clusters of $CF_3O^-$ with hydroxyhydroperoxides, produced from the oxidation of simple alkenes, fragment to *m/z* = 63, whereas those with BEPOX exhibit loss of hydrofluoric acid (HF). The daughter *m/z* = 63 of 203 (Fig. 1, green curve), associated with the fragmentation of the ISOPOOH cluster clearly precedes the daughter *m/z* = 183 of 203 (Fig. 1, blue curve), associated with IEPOX, consistent with the proposed mechanism. Clusters of $CF_3O^-$ with other plausible isomers of IEPOX are not known to exhibit efficient loss of HF (*13*). The sum of the *m/z* = 63 and *m/z* = 183 daughters (Fig. 1, black dashed line) properly captures the shape of the parent signal (Fig. 1, red curve).

Experiments performed with $^{18}OH$ produced from the photolysis of $H^{18}O^{18}OH$ provide additional evidence for the conversion of ISOPOOH to IEPOX. With $^{18}OH$ as the primary oxidant, ISOPOOH and IEPOX are no longer isobaric: The ISOPOOH ion cluster is primarily monitored at *m/z* = 205 (Fig. 2, magenta circles) corresponding to the addition of one $^{18}OH$ on isoprene (Reaction Series 1, A and B), whereas IEPOX is detected at *m/z* = 207 (Fig. 2, blue squares) because its formation requires addition of a second $^{18}OH$ and simultaneous loss of $^{16}OH$ (Reaction Series 2, A and B) (Fig. 2). The coincidence between *m/z* = 207 and IEPOX fingerprint (daughter *m/z* = 187) suggests that *m/z* = 207 is derived almost entirely from the dilabeled IEPOX, consistent with the proposed mechanism.

Quantum chemical calculations confirm that, after the addition of OH, ISOPOOH is connected to IEPOX by energetically favorable adiabatic pathways (Fig. 3 and tables S4 and S5). β- and δ-IEPOX lie ~50 kcal/mol below their ISOPOOH parent with the transition state connecting the alkyl radical and IEPOX ~20 kcal/mol below the ISOPOOH reactant. The relative energies and structures of the stationary points along the surface are shown in Fig. 3 for the β4-ISOPOOH to β-IEPOX reaction (Reaction Series 2A). The reaction paths and energetics for the analogous β1-ISOPOOH to β-IEPOX reaction and for the δ4-ISOPOOH to δ4-IEPOX reaction (Reaction Series 2B) are similar (figs. S3 and S4 and tables S6 and S7).

The formation of isotopically light ISOPOOH (*m/z* = 203) (Fig. 2, red circles) and IEPOX (*m/z* = 203 and 205) (Fig. 2, red and magenta squares) in the $^{18}OH$-labeled experiment provides additional evidence for Reaction Series 2, A and B, because $^{16}OH$ is released through formation of IEPOX (Reaction Series 2, A and B). The $^{16}OH$ quickly reacts with isoprene and ISOPOOH, forming the observed isotopically light compounds. The formation of light ISOPOOH (*m/z* = 203) in the first hour of the experiment cannot, however, be accounted for by Reaction Series 2, A and B, alone, suggesting a small but rapid $^{16}OH$ formation from Reaction Series 1C. This is consistent with the coincident production of MVK and MACR, measured together by proton transfer mass spectrometry at *m/z* = 89. Very little methyl-butenediol (<2%) is observed, which suggests that cross-peroxy radical reactions (*23*) are unlikely to account for the formation of MVK and MACR. A prompt signal at *m/z* = 201 appears consistent with the recently hypothesized

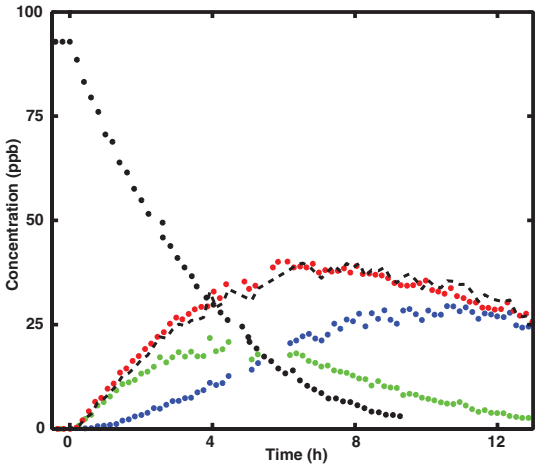


**Fig. 1.** Consecutive formation of ISOPOOH and IEPOX in the photooxidation of isoprene. Following the time when the photolysis of $H_2O_2$ [initially 1.66 parts per million by volume (ppmv)] begins (*t* = 0), isoprene (black dotted line) decays quickly. ISOPOOH and then IEPOX are detected as major products of the oxidation of isoprene [because they are isobaric, they both are detected at *m/z* = 203 (red), the cluster of these compounds with $CF_3O^-$]. Tandem mass spectroscopy provides for separation of the *m/z* = 203 signal: ISOPOOH (green) is observed as the *m/z* = 63 daughter, whereas IEPOX (blue) is observed as the *m/z* = 183 daughter. The sum of IEPOX and ISOPOOH is indicated by the dashed black line.

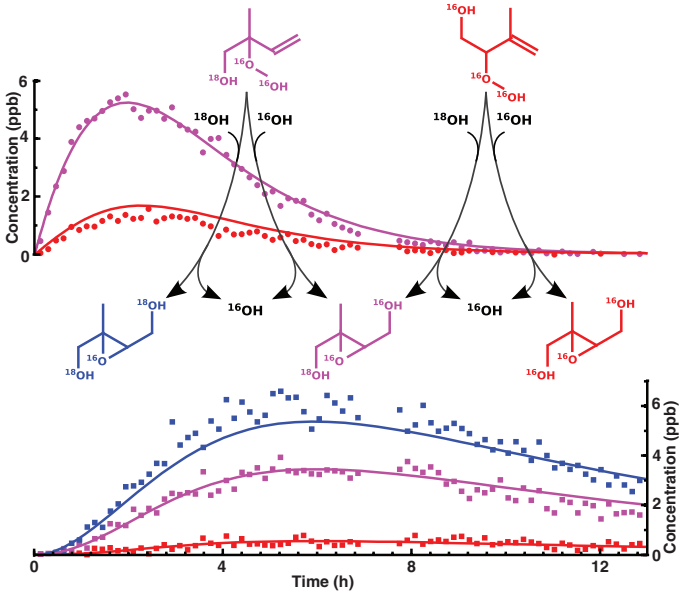


**Fig. 2.** Formation of light and heavy ISOPOOH and IEPOX in the oxidation of isoprene using $H^{18}O^{18}OH$ as the OH source. Formation of ISOPOOH is monitored via the daughter *m/z* = 63 (circles) of *m/z* = 203 (red) and *m/z* = 205 (magenta). Formation of IEPOX is monitored via the loss of HF (squares) from *m/z* = 203, *m/z* = 205, and *m/z* = 207 (blue). Formation of isotopically light ISOPOOH and IEPOX reflects OH reformation. Solid lines represent the modeled mixing ratios for the different isomers. Isoprene initial concentration was 23.5 parts per billion by volume (ppbv), and $^{18}OH$ was generated from the photolysis of $H^{18}O^{18}OH$ (1.75 ppmv initial concentration, UV lights on at *t* = 0).

Downloaded from http://science.sciencemag.org/ on January 15, 2017

formation of (2Z)-hydroperoxymethylbutenol by a 1,6 H shift. However, its yield (<10% of ISOPOOH) is much less than predicted theoretically (*14*).

Using a kinetic model constrained by the observed yields of MVK/MACR and the ratios between light and heavy isotopes of ISOPOOH, we estimate that 12 ± 12% of the isoprene peroxy radicals react with $HO_2$ to recycle OH by Reaction 1C. This estimate accounts for a small initial amount of $NO_x$ present initially in the chamber (*13*). The balance of the isoprene peroxy radicals reacts with $HO_2$ to form ISOPOOH.

The lifetime of ISOPOOH with respect to OH (3 to 5 hours) is considerably shorter than IEPOX (18 to 22 hours) (calculated for [OH] = $10^6$ radicals $cm^{-3}$). The formation of unlabeled hydroxyacetone as well as singly labeled hydroxyacetone and glycolaldehyde in the photooxidation of isoprene by $^{18}OH$ suggests that the degradation of IEPOX by OH occurs primarily through hydrogen abstraction α to the alcohol (*13*).

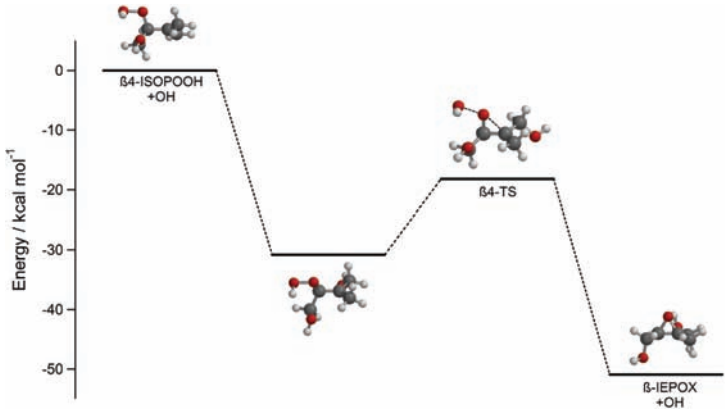


**Fig. 3.** Relative energies for the formation of β-IEPOX from β4-ISOPOOH (Reaction Series 2A). The alkylradical resulting from the addition of OH onto β4-ISOPOOH double bond is formed with enough excess energy (~30 kcal/mol) that it quickly decomposes to the β-IEPOX + OH via the β4-transition state. Energies are calculated with the CCSD(T)-F12/VDZ-F12 explicitly correlated method at the B3LYP/cc-pVTZ optimized structures (*13*).

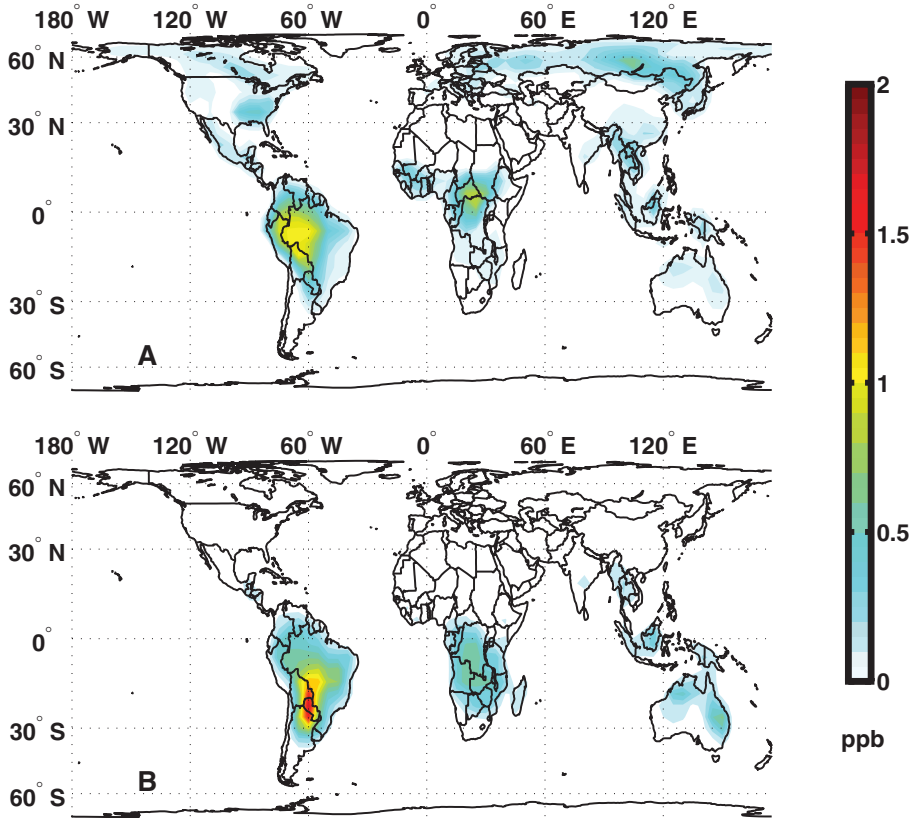


**Fig. 4.** Simulated daily distribution of IEPOX in the planetary boundary layer during the Northern Hemisphere summer (**A**) and winter (**B**). IEPOX seasonal cycle mirrors the isoprene emissions. The mixing ratio of IEPOX is higher in the tropics than in other isoprene production regions in the northern mid-latitudes (e.g., the southeast United States). This reflects the reduction in the yield of IEPOX from isoprene due to anthropogenic emissions of NO.

In addition to the gas-phase oxidation, dihydroxyepoxides are lost to aerosol surfaces through reactive uptake. We monitor by CID-CIMS rapid and nearly quantitative uptake of BEPOX onto acidic aerosol seeds ($MgSO_4/H_2SO_4$). The resulting SOA composition can be readily related to the one identified for *i*SOA in pristine environments. In particular, analogs of dihydroxyenols, 2-methyltetrols, alkene-triols, and associated sulfate esters are detected (*13*), which suggests that IEPOX may explain their formation in both field (*7*, *24*) and chamber studies (*17*, *18*). Epoxides are also known to polymerize easily, an essential process for SOA growth (*25*).

The atmospheric yield of IEPOX is directly related to the relative importance of the reactions of isoprene peroxy radicals with $HO_2$ and NO. Using the chemical transport model GEOS-CHEM (*26*) with an updated chemical mechanism (table S9) (*21*), we find that globally about one-third of isoprene peroxy radicals undergo reaction with $HO_2$, with the remaining fraction reacting with NO. Over the Amazon, this ratio is almost inverted (fig. S7). Including uncertainties in isoprene emissions, we estimate that 95 ± 45 Tg C/year of IEPOX, a previously unknown class of compounds, are formed each year in the atmosphere. The largest concentrations of IEPOX are localized over the southern tropics, with substantial levels predicted over Canada and the Southeast United States during Northern Hemisphere summer (Fig. 4).

The presence of high concentrations of ISOPOOH and IEPOX in the atmosphere are consistent with recent aircraft-borne observations of isoprene oxidation products ($m/z$ = 203) over southeast Columbia [NASA Tropical Composition, Cloud, and Climate Coupling (TC4) campaign] and ($m/z$ = 203 and its daughters) over Alberta and California [NASA Artic Research of the Composition of the Troposphere from Aircraft and Satellites (ARCTAS) campaign]. Preliminary study of the data collected in the boundary layer is consistent with the concentrations of these compounds calculated with GEOS-CHEM (fig. S8).

The variability in the yield and fate of IEPOX is expected to translate into highly variable *i*SOA yields. In particular, anthropogenic activities depress for IEPOX formation as IEPOX yield drops rapidly with increasing NO. Anthropogenic emissions, however, may enhance the *i*SOA yield from IEPOX because its uptake on surfaces is likely dependent on the aerosol pH and sulfur content (*19*, *27*). This may explain part of the variability of the reported SOA biogenic yields, ranging from negligible (*28*) to potentially dramatic (*29*). Given the enormous flux of IEPOX, the chemistry presented here may also resolve part of the intriguing discrepancy between bottom-up

Downloaded from http://science.sciencemag.org/ on January 15, 2017

(10 to 70 Tg/year) and top-down (140 to 910 Tg/year) estimates of global SOA production (*30*). Nevertheless, IEPOX is expected to undergo hundreds of collisions with aerosol surfaces before reacting with OH, and its detection in the atmosphere (fig. S8) suggests that a complex suite of conditions likely controls its uptake to aerosols (e.g., the pH and chemical composition of aerosol). Furthermore, *i*SOA formation may depend on the unquantified differences in the yields and uptake characteristics of the β- and δ-IEPOX. Quantitative understanding of these complex interactions is required to assess the effect of this chemistry on the overall SOA abundance and its associated impacts [e.g., cloud condensation nuclei (*31*)].

The efficient formation of dihydroxyepoxides, a previously unknown class of gas-phase compounds, addresses many of the issues currently being debated about isoprene chemistry. Because their formation is accompanied by the reformation of OH, this chemistry contributes to the remarkable stability of $HO_x$ in remote regions of the troposphere subjected to high isoprene emissions. The formation of IEPOX also provides a gas-phase precursor for the *i*SOA formation. Further investigation of the multiphase chemistry of IEPOX is needed to elucidate the complex interaction between emissions from the biosphere and atmospheric composition (*32*, *33*). In particular, the development of a proper chemical description of these interactions is essential for assessing the sensitivity of this chemistry to changes in isoprene emissions caused by environmental changes (e.g., climate change and deforestation) and to the further development of anthropogenic activities and the accompanying $NO_x$ emissions in these regions.

**References and Notes**


1. A. Guenther *et al.*, *Atmos. Chem. Phys.* **6**, 3181 (2006).
2. P. C. Harley, R. K. Monson, M. T. Lerdau, *Oecologia* **118**, 109 (1999).
3. J. D. Fuentes *et al.*, *Bull. Am. Meteorol. Soc.* **81**, 1537 (2000).
4. T. N. Rosenstiel, M. J. Potosnak, K. L. Griffin, R. Fall, R. K. Monson, *Nature* **421**, 256 (2003).
5. C. Wiedinmyer, X. Tie, A. Guenther, R. Neilson, C. Granier, *Earth Interact.* **10**, 1 (2006).
6. R. von Kuhlmann, M. G. Lawrence, U. Pöschl, P. J. Crutzen, *Atmos. Chem. Phys.* **4**, 1 (2004).
7. M. Claeys *et al.*, *Science* **303**, 1173 (2004).
8. P. Crutzen *et al.*, *Atmos. Environ.* **34**, 1161 (2000).
9. C. E. Reeves, S. A. Penkett, *Chem. Rev.* **103**, 5199 (2003).
10. J. A. Thornton *et al.*, *J. Geophys. Res.* **107**, 17 (2002).
11. J. Lelieveld *et al.*, *Nature* **452**, 737 (2008).
12. X. Ren *et al.*, *J. Geophys. Res.* **113**, 5310 (2008).
13. Materials and methods are available as supporting material on *Science* Online.
14. J. Peeters, T. L. Nguyen, L. Vereecken, *Phys. Chem. Chem. Phys.*, **11**, 5935 (2009).
15. T. J. Dillon, J. N. Crowley, *Atmos. Chem. Phys.* **8**, 4877 (2008).
16. E. R. Bell, F. F. Rust, W. E. Vaughan, *J. Am. Chem. Soc.* **72**, 337 (1950).
17. W. Wang *et al.*, *Rapid Commun. Mass Spectrom.* **19**, 1343 (2005).
18. J. D. Surratt *et al.*, *J. Phys. Chem. A* **110**, 9665 (2006).
19. E. C. Minerath, M. J. Elrod, *Environ. Sci. Technol.* **43**, 1386 (2009).
20. J. D. Crounse, K. A. McKinney, A. J. Kwan, P. O. Wennberg, *Anal. Chem.* **78**, 6726 (2006).
21. F. Paulot *et al.*, *Atmos. Chem. Phys.* **9**, 1479 (2009).
22. F. W. McLafferty, *Science* **214**, 280 (1981).
23. L. Ruppert, K. H. Becker, *Atmos. Environ.* **34**, 1529 (2000).
24. J. D. Surratt *et al.*, *J. Phys. Chem. A* **112**, 8345 (2008).
25. S. Gao *et al.*, *Environ. Sci. Technol.* **38**, 6582 (2004).
26. I. Bey *et al.*, *J. Geophys. Res.* **106**, 73 (2001).
27. J. D. Surratt *et al.*, *Environ. Sci. Technol.* **41**, 5363 (2007).
28. J. A. de Gouw *et al.*, *J. Geophys. Res.* **110**, D16305 (2005).
29. P. Tunved *et al.*, *Science* **312**, 261 (2006).
30. A. H. Goldstein, I. E. Galbally, *Environ. Sci. Technol.* **41**, 1515 (2007).
31. V.-M. Kerminen, H. Lihavainen, M. Komppula, Y. Viisanen, M. Kulmala, *Geophys. Res. Lett.* **32**, L14803 (2005).
32. F. W. Went, *Nature* **187**, 641 (1960).
33. M. O. Andreae, P. J. Crutzen, *Science* **276**, 1052 (1997).


34. We thank X. Levine, H. O. T. Pye, and the Harvard GEOS CHEM team (Daniel J. Jacob, principal investigator) for their help in setting up the GEOS-CHEM model; A. J. Kwan, A. W. Chan, P. S. Chhabra, and N. Eddingsaas for experimental assistance; J. D. Surratt for providing the speciation of the SOA resulting from BEPOX reactive uptake; and J. Lane, I. Maxwell-Cameron, and S. Jørgensen for helpful discussions regarding the quantum calculations. F.P. was partially supported by the William and Sonya Davidow fellowship. J.D.C. thanks the EPA Science to Achieve Results (STAR) Fellowship Program (FP916334012) for providing partial support. The mass spectrometer used in this study was purchased as part of a major research instrumentation grant from the National Science Foundation (ATM-0619783). Assembly and testing of the CIMS instrument was supported by the Davidow Discovery Fund. The numerical simulations for this research were performed on Caltech's Division of Geological and Planetary Sciences Dell Cluster. This work was supported by the Office of Science (Biological and Environmental Research), U.S. Department of Energy grant DE-FG02-05ER63983, U.S. Environmental Protection Agency STAR agreement RD-833749, and the Marsden Fund administrated by the Royal Society of New Zealand. The TC4 and ARCTAS campaigns were supported by NASA grants NNX07AL33G and NNX08AD29G. This work has not been formally reviewed by the EPA. The views expressed in this document are solely those of the authors, and the EPA does not endorse any products or commercial services mentioned in this publication.


**Supporting Online Material**
www.sciencemag.org/cgi/content/full/325/5941/730/DC1
Materials and Methods
Figs. S1 to S9
Tables S1 to S9
References

2 March 2009; accepted 24 June 2009
10.1126/science.1172910

Downloaded from http://science.sciencemag.org/ on January 15, 2017

# Phylogenetic Conservatism of Extinctions in Marine Bivalves

**Kaustuv Roy,[1]* Gene Hunt,[2] David Jablonski[3]**

**Evolutionary histories of species and lineages can influence their vulnerabilities to extinction, but the importance of this effect remains poorly explored for extinctions in the geologic past. When analyzed using a standardized taxonomy within a phylogenetic framework, extinction rates of marine bivalves estimated from the fossil record for the last ~200 million years show conservatism at multiple levels of evolutionary divergence, both within individual families and among related families. The strength of such phylogenetic clustering varies over time and is influenced by earlier extinction history, especially by the demise of volatile taxa in the end-Cretaceous mass extinction. Analyses of the evolutionary roles of ancient extinctions and predictive models of vulnerability of taxa to future natural and anthropogenic stressors should take phylogenetic relationships and extinction history into account.**

Groups of organisms differ in their vulnerability to extinction (*1*–*5*), but the nature and magnitude of that variation is still poorly quantified. Extinction risk of species and lineages is determined by a variety of ecological and life history traits (*2*), as well as emergent properties such as geographic range (*5*–*8*). Many of these extinction-related traits are phylogenetically conserved, suggesting that extinctions should be phylogenetically clustered: Taxa in some clades should be consistently more extinction-prone than others (*3*, *9*, *10*). Consistent with this idea, current extinction risk and documented anthropogenic extinctions are nonrandomly distributed among vertebrate lineages (*9*, *11*–*15*), but whether such phylogenetic selectivity holds in general, including for extinctions in the geologic past, remains poorly known. In this study, we used the Mesozoic-Cenozoic fossil record of marine bivalves, in conjunction with molecular phylogenies, to test for phylogenetic clustering of extinctions within and among bivalve families and how this clustering varies over time.

The fossil record of marine bivalves preserves a rich history of past extinctions, and although this record is not free of taphonomic biases, such biases are increasingly well understood (*16*, *17*). We used a taxonomically standardized database

[1]Section of Ecology, Behavior and Evolution, University of California San Diego, La Jolla, CA 92093–0116, USA. [2]Department of Paleobiology, National Museum of Natural History, Smithsonian Institution, Washington, DC 20013–7012, USA. [3]Department of Geophysical Sciences, University of Chicago, 5734 South Ellis Avenue, Chicago, IL 60637, USA.

*To whom correspondence should be addressed. E-mail: kroy@ucsd.edu

EXTENDED PDF FORMAT
SPONSORED BY

www.rndsystems.com

Science
AAAS

**Unexpected Epoxide Formation in the Gas-Phase Photooxidation of Isoprene**

Fabien Paulot, John D. Crounse, Henrik G. Kjaergaard, Andreas Kürten, Jason M. St. Clair, John H. Seinfeld and Paul O. Wennberg

(August 6, 2009)
*Science* **325** (5941), 730-733. [doi: 10.1126/science.1172910]

Editor's Summary

**No NO**

Isoprene, a five-carbon diene produced by plants, is the most abundant nonmethane hydrocarbon released into the atmosphere and plays an important role in tropospheric chemistry. Isoprene is also thought to affect climate by acting as a source of atmospheric aerosols. **Paulot *et al.*** (p. 730; see the Perspective by **Kleindienst**) now describe how isoprene may lead to the formation of secondary organic aerosols. In laboratory experiments, the photooxidation of isoprene in low-NO conditions, such as those which occur in vegetated regions far from anthropogenic influence, produced high yields of dihydroxy epoxides, a suspected precursor of the aerosols. This discovery could help to explain some of the more puzzling aspects of isoprene chemistry in remote regions.

This copy is for your personal, non-commercial use only.

**Article Tools** Visit the online version of this article to access the personalization and article tools:
http://science.sciencemag.org/content/325/5941/730

**Permissions** Obtain information about reproducing this article:
http://www.sciencemag.org/about/permissions.dtl

*Science* (print ISSN 0036-8075; online ISSN 1095-9203) is published weekly, except the last week in December, by the American Association for the Advancement of Science, 1200 New York Avenue NW, Washington, DC 20005. Copyright 2016 by the American Association for the Advancement of Science; all rights reserved. The title *Science* is a registered trademark of AAAS.

Downloaded from http://science.sciencemag.org/ on January 15, 2017